論 文

THE EFFECTS OF ALLOYING ELEMENTS AND COOLING RATES DURING SOLIDIFICATION ON THE MICROSTRUCTURE AND MECHANICAL PROPERTIES OF P-CONTAINED C/V GRAPHITE CAST IRONS

Myung-Ho Kim, Heung-Il Park*, Woo-Yeol Kim* and Cha-Hurn Bae*

DER EINFLUSS VON LEGIERUNGSELEMENTE UND ABKÜHLUNGSGESCHWINDIGKEIT WAHREND DER ERSTARRUNG AUF DIE MIKROSTRUKTUR UND MECHANISCHE EIGENSCHAFTEN VON P-HALTIGEN GGV

LES EFFETS DES ÉLEMENTS D'ALLIAGE ET DE TAUX DE REFROIDISSEMENT PENDANT SOLIDIFICATION SUR LA MICROSTRUCTURE ET PROPRIÉTÉ MÉCANIQUE DE FONTES GRISES PHOSPHOREES AVEC DU GRAPHITE COMPACTE/VERMICULAIRE

Summary.

This study was undertaken to obtain an improved understanding of the effects of alloying elements on the residual amounts of Mg in the melt and on the resultant microstructure of compacted vermicular graphite cast irons, and the influence of alloying elements and cooling rates during solidification on the formation of phosphide eutectics, and on the mechanical properties of compacted vermicular graphite cast irons containing copper, tin, molybdenum for producing pearlitic matrix, and also containing phosphorus and boron for increasing wear resistance were evaluated.

1. INTRODUCTION

Recently, it has become of importance to reduce the oil consumption and to improve the engine performance in the design of marine diesel engines, of which cylinder liners are usually made with flake graphite cast irons. As one of the most effective measures for this is to increase the combustion pressure, the requirements for the material strength of the cylinder liners have been increased[1-5]. Cylinder liner materials represent a compromise between the wear properties required and the mechanical properties to withstand the differential thermal stresses which are cyclically applied. By modifying the

Department of Metallurgical Engineering, Inha University, Inchon 402-751, Korea
*Department of Production & Joining Engineering, Pusan National University of Technology, Pusan 608-739, Korea

본 논문은 중국 북경에서 개최된 61차 국제주물대회에서 한국대표논문으로 발표된 내용임.

graphite morphology of the cast iron from flake to compacted-vermicular type, the tensile, elongation and impact properties of the cast irons can be improved without loss in thermal conductivity, damping capacity and machinability[6-15], and the metallographic constituents of the cast iron have been shown to be of prime importance in controlling the wear properties[16-20]. Therefore, in the production process of high strength, highly wear resistant compacted vermicular graphite cast irons with a reduced magnesium treatment method, control of processing variables and combination of alloying elements to obtain a desired graphite structure and matrix structure are very important.

In this study, the influence of alloying elements and cooling rates during solidification on the formation of phosphide eutectics, and on the mechanical properties of CV graphite cast irons containing copper, tin, molybdenum for producing pearlitic matrix, and also containing phosphorus and boron for increasing wear resistance, were investigated.

2. EXPERIMENTAL

All heats were prepared in a 25kgs induction furnace(50 kw, 3 kHz) having a magnesia crucible and were made up from charges of low sulfur pig iron to which necessary additions of manganese, molybdenum, copper, phosphorus, boron, silicon and carbon were made with commercial ferro-alloys, graphite and copper wire. The melt was heated to 1500℃ and the base iron chemistry was checked using chemical analysis by emission spectrometer(Shimadzu, GVM-514). When the desired chemistry was attained, the melt was treated with Fe-45%Si-4.5%Mg by use of sandwich ladles. All heats were post-inoculated with 0.2% Ca-Si alloy, and poured at 1350-1370℃.

For investigating the effects of phosphorus and boron on the formation of graphite structure, after the treatment the melt was poured back into the furnace and the melt temperature was lowed and held at 1350℃ for 20 minutes, taking samples at every minutes. Samples of bar type(30mm in diameter and 150mm in height) were cast in sand mold for microstructural observations, and chilled disk specimens were prepared for chemical analysis. The area fraction of the graphite and phosphide eutectics were examined with particle analyzer(Nihon Regurator Co, LUZEX 450).

3. RESULTS AND DISCUSSIONS

3.1 The effects of P and B on the graphite structure

A heat with basic chemical composition (heat A), a heat with addition of 0.2% P (heat B), a heat with addition of both 0.2% P and 0.035% B(heat C), and a heat with 0.035% B(heat D) were prepared for this study. After the treatment with Fe-45%Si-4.5%Mg, the melt was held at 1350 C for 20 minutes, taking samples at every minutes. The chemical composition and graphite morphology of the samples examined are presented in Table 1.

Fig.1 (a) and (b) display the variation of the recovery ratio of residual magnesium and sulfur content with holding time at constant temperature, respectively. It is evident that the recovery ratio of residual magnesium content was consistantly decreased with holding time, and the fading of residual magnesium in the melt with phosphorus(heat B) was slower than in the melt with boron(heat C & D). This is mainly due to the fact that in this experiment phosphorus was added 23 times more in moles than boron, thus the residual oxygen content of the melt with

Table 1. Changes in chemical compositions and graphite morphology with holding time.

Heat A (Base melt) **Heat B (Base melt containing 0.2%P)**

Holding time (min.)	Chemical composition							Graphite morphology	Holding time (min.)	Chemical composition							Graphite morphology
	C	Si	Mn	P	S	B	Mg			C	Si	Mn	P	S	B	Mg	
0	4.05	1.64	0.67	0.0319	0.0066	-	0.0327	N	0	3.74	1.61	0.70	0.1744	0.0110	-	0.0365	N
1	4.00	1.64	0.66	0.0315	0.0054	-	0.0303	N	1	3.64	1.58	0.66	0.1588	0.0119	-	0.0336	N
2	4.04	1.62	0.66	0.0323	0.0064	-	0.0315	N	2	3.68	1.59	0.68	0.1684	0.0105	-	0.0305	N
3	3.96	1.61	0.65	0.0321	0.0040	-	0.0217	N	3	3.66	1.58	0.67	0.1626	0.0090	-	0.0265	N
4	4.00	1.62	0.68	0.0327	0.0051	-	0.0265	N	4	3.70	1.57	0.67	0.1695	0.0085	-	0.0251	N
5	4.00	1.61	0.65	0.0308	0.0032	-	0.0247	N	5	3.67	1.58	0.70	0.1610	0.0045	-	0.0198	N
6	3.96	1.63	0.67	0.0327	0.0042	-	0.0242	N	6	3.68	1.57	0.68	0.1698	0.0035	-	0.0172	N
7	3.94	1.60	0.63	0.0280	0.0009	-	0.0206	N	7	3.74	1.57	0.69	0.1694	0.0037	-	0.0167	N
8	3.99	1.60	0.66	0.0319	0.0017	-	0.0208	N	8	3.71	1.58	0.68	0.1648	0.0023	-	0.0153	N
9	3.99	1.61	0.66	0.0315	0.0017	-	0.0169	N	9	3.68	1.56	0.67	0.1678	0.0031	-	0.0154	N
10	4.07	1.59	0.66	0.0327	0.0025	-	0.0179	N+CV	10	-	-	-	-	-	-	-	N
11	3.99	1.61	0.66	0.0330	0.0023	-	0.0179	N+CV	11	3.61	1.55	0.66	0.1549	0.0012	-	0.0117	N+CV
12	4.03	1.58	0.66	0.0317	0.0014	-	0.0135	N+CV	12	3.73	1.56	0.68	0.1618	0.0029	-	0.0110	CV
13	3.99	1.60	0.65	0.0312	0.0018	-	0.0144	N+CV	13	3.62	1.57	0.67	0.1625	0.0019	-	0.0096	CV
14	4.03	1.61	0.66	0.0334	0.0022	-	0.0126	CV	14	3.66	1.56	0.67	0.1683	0.0032	-	0.0096	CV
15	4.01	1.59	0.65	0.0318	0.0019	-	0.0123	CV	15	3.62	1.55	0.68	0.1624	0.0026	-	0.0078	CV
16	4.03	1.58	0.67	0.0326	0.0033	-	0.0124	CV	16	3.62	1.56	0.67	0.1661	0.0029	-	0.0076	CV
17	3.94	1.58	0.65	0.0315	0.0014	-	0.0102	CV	17	3.64	1.54	0.67	0.1633	0.0030	-	0.0066	CV
18	3.94	1.59	0.64	0.0308	0.0011	-	0.0097	CV	18	3.60	1.53	0.68	0.1658	0.0029	-	0.0054	CV
19	4.03	1.58	0.67	0.0342	0.0027	-	0.0092	CV	19	3.67	1.54	0.68	0.1623	0.0041	-	0.0050	CV
20	4.06	1.58	0.67	0.0346	0.0036	-	0.0084	CV	20	3.66	1.54	0.67	0.1695	0.0050	-	0.0048	CV

Heat C (Base melt containing 0.2%P and 0.035%B) **Heat D (Base melt containing 0.035%B)**

Holding time (min.)	Chemical composition							Graphite morphology	Holding time (min.)	Chemical composition							Graphite morphology
	C	Si	Mn	P	S	B	Mg			C	Si	Mn	P	S	B	Mg	
0	3.63	1.65	0.66	0.1618	0.0192	0.0324	0.0455	N	0	3.75	1.68	0.66	0.0377	0.0190	0.0323	0.0399	N
1	3.67	1.59	0.65	0.1600	0.0170	0.0319	0.0313	N	1	3.70	1.68	0.67	0.0391	0.0221	0.0324	0.0371	N+CV
2	3.63	1.62	0.66	0.1651	0.0129	0.0322	0.0270	N	2	3.70	1.68	0.66	0.0393	0.0132	0.0318	0.0240	N+CV
3	-	-	-	-	-	-	-	N	3	3.74	1.69	0.66	0.0391	0.0187	0.0333	0.0253	N+CV
4	3.56	1.61	0.65	0.1623	0.0071	0.0318	0.0172	N+CV	4	3.70	1.66	0.66	0.0384	0.0096	0.0328	0.0128	CV
5	3.51	1.59	0.63	0.1518	0.0054	0.0307	0.0148	CV	5	3.61	1.68	0.66	0.0384	0.0093	0.0324	0.0130	CV
6	3.63	1.60	0.67	0.1632	0.0040	0.0318	0.0101	CV	6	3.72	1.66	0.67	0.0385	0.0092	0.0329	0.0086	CV
7	3.62	1.58	0.66	0.1602	0.0044	0.0318	0.0099	CV	7	3.72	1.64	0.66	0.0389	0.0070	0.0326	0.0066	CV
8	3.45	1.60	0.64	0.1528	0.0040	0.0310	0.0087	CV	8	3.68	1.65	0.65	0.0370	0.0061	0.0324	0.0047	F
9	3.70	1.56	0.68	0.1619	0.0048	0.0326	0.0072	CV	9	3.74	1.64	0.67	0.0383	0.0063	0.0328	0.0036	F
10	3.52	1.60	0.66	0.1649	0.0051	0.0318	0.0068	CV	10	3.70	1.65	0.66	0.0377	0.0081	0.0327	0.0036	F
11	3.58	1.59	0.66	0.1690	0.0045	0.0312	0.0057	CV	11	3.68	1.64	0.65	0.0383	0.0073	0.0328	0.0028	F
12	3.57	1.58	0.65	0.1620	0.0039	0.0317	0.0045	CV	12	3.70	1.64	0.67	0.0387	0.0075	0.0325	0.0025	F
13	3.55	1.59	0.65	0.1615	0.0044	0.0320	0.0041	F	13	3.54	1.64	0.65	0.0334	0.0067	0.0323	0.0023	F
14	3.59	1.60	0.66	0.1660	0.0057	0.0317	0.0036	F	14	-	-	-	-	-	-	-	F
15	3.54	1.59	0.66	0.1558	0.0056	0.0324	0.0032	F	15	3.64	1.63	0.66	0.0380	0.0112	0.0329	0.0022	F
16	3.55	1.58	0.67	0.1640	0.0067	0.0320	0.0029	F	16	3.66	1.63	0.66	0.0362	0.0082	0.0329	0.0021	F
17	3.51	1.59	0.66	0.1586	0.0074	0.0323	0.0026	F	17	3.59	1.63	0.66	0.0367	0.0117	0.0326	0.0021	F
18	3.49	1.57	0.65	0.1577	0.0078	0.0314	0.0024	F	18	3.63	1.61	0.65	0.0367	0.0127	0.0322	0.0020	F
19	3.32	1.55	0.62	0.1377	0.0050	0.0308	0.0022	F	19	3.61	1.63	0.66	0.0384	0.0135	0.0328	0.0021	F
20	3.52	1.58	0.65	0.1601	0.0104	0.0321	0.0021	F	20	3.66	1.61	0.68	0.0397	0.0156	0.0334	0.0020	F

* N : nodular graphite
CV : compacted vermicular graphite
F : flake graphite

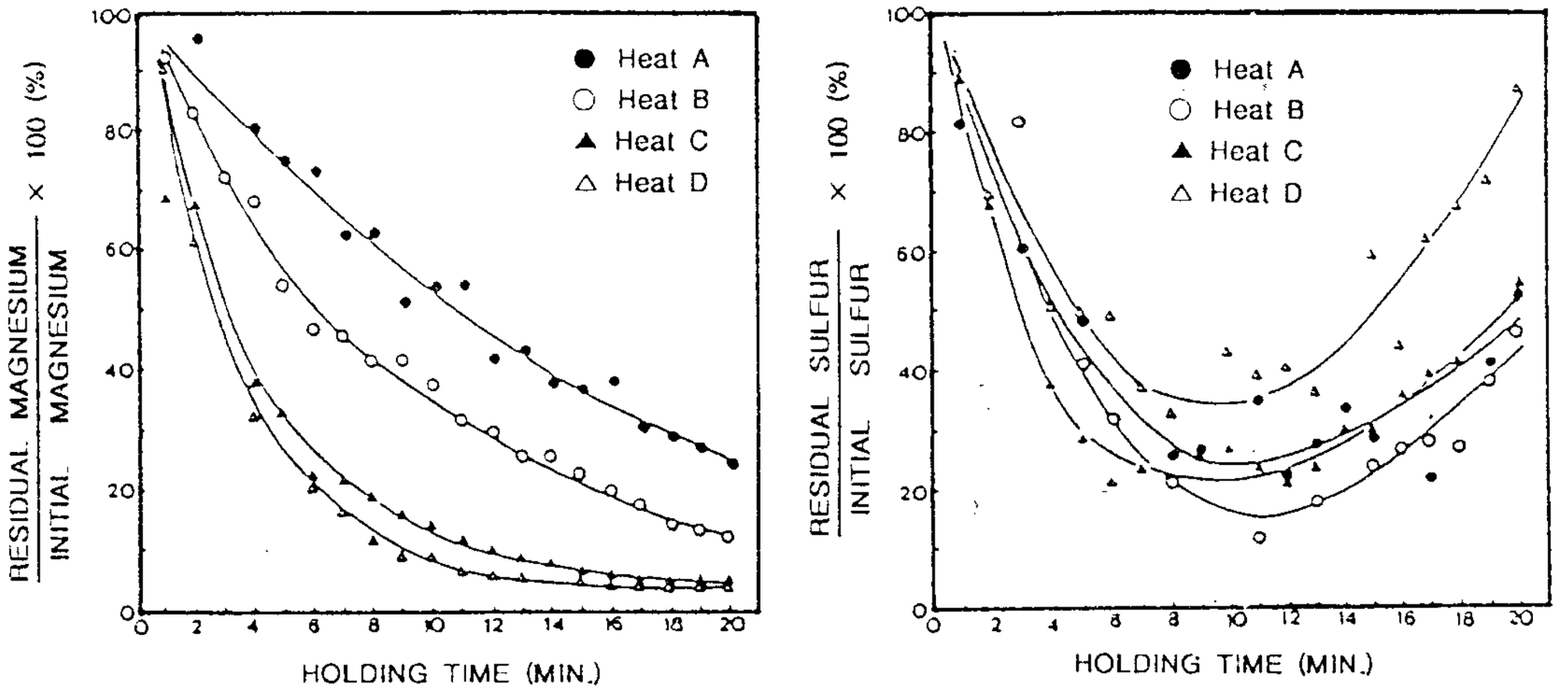

Fig. 1. Changes in the recovery ratio of (a) residual Mg contents, and (b) residual S content with isothermal holding time.

phosphorus was much lower than the melt with boron, as they could easily form P_2O_5 and B_2O_3 in the melt, respectively. Therefore, the fading of magnesium by formation of magnesium oxide for the melt with phosphorus should be slower than the melt with boron.

However, the recovery ratio of residual sulfur content was decreased at the begining stage, but later increased again with holding time, i. e. sulfur reversions were happened. Such a sulfur reversion is attributed to the excess delay without removal of the reaction products (i.e. magnesium sulfide) from the liquid iron surface, as the magnesium sulfides react with the oxygen in the atmosphere [21,22].

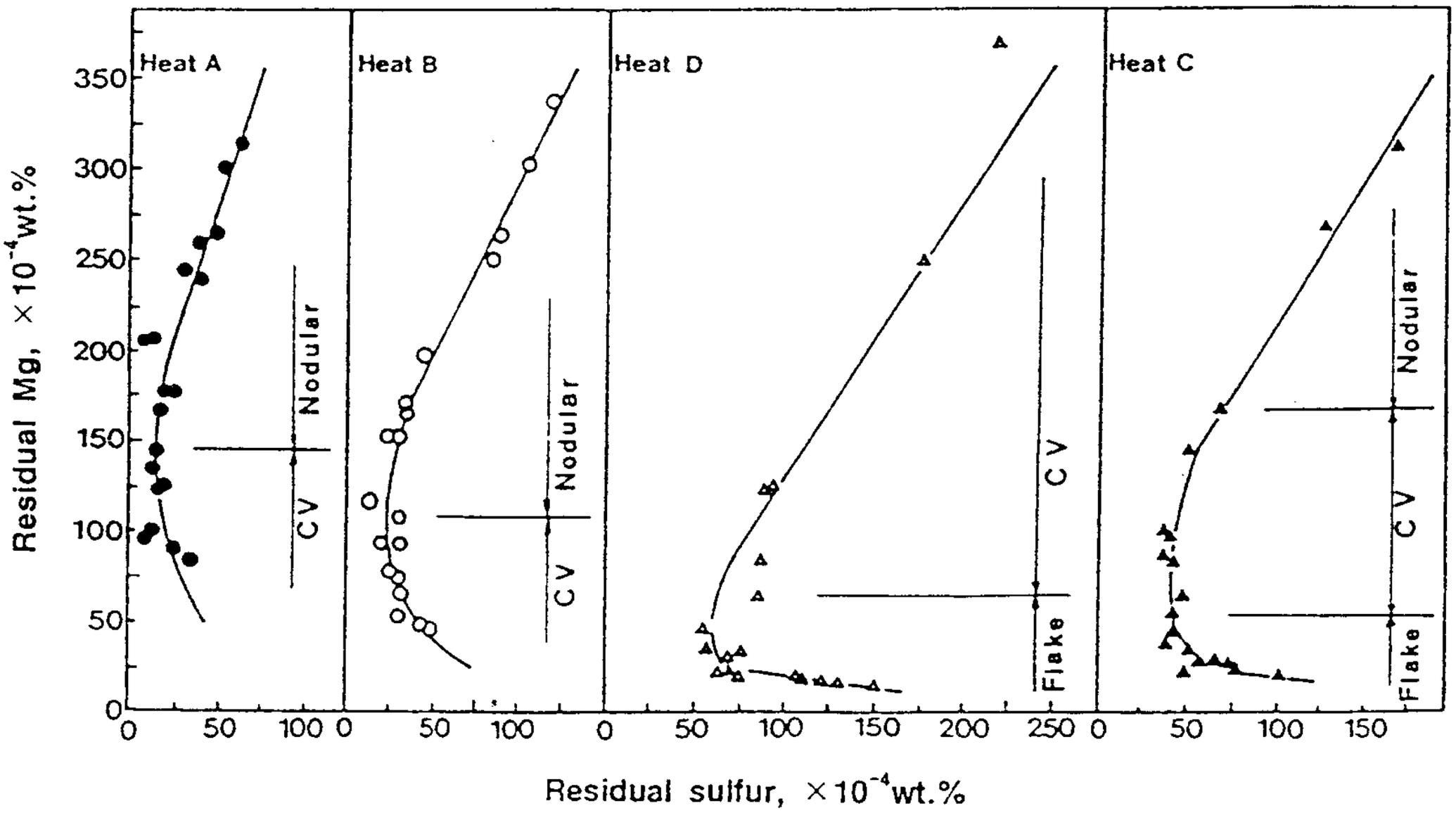

Fig. 2. Relation between the variation of Mg contents and S contents during isothermal holding.

The melt with boron shows higher sulfur reversion than the melt with phosphorus, and this is due to the fact that P_2O_3 increase the sulfide capacity of the slag and dross[23]. Change in residual content of Mg and sulfur in the melt with time can be displayed in C-curve, as shown in Fig.2, and these figures show that the nose of C-curve is shifted to the direction of decreasing Mg content and increasing sulfur content by addition of boron and phosphorus in the melt. Fig.2 also shows the effect of magnesium-sulfur interaction on the graphite morphology of cast irons during isothermal holding.

Fig.3 shows the variation of graphite morphology with the Mg-Equivalent(=residual% Mg-3/4 residual%S). A compacted vermicular graphite structure was produced for heat A when the Mg-Equivalent was less than 0.0161, and the Mg-Equivalent for producing compacted vermicular graphite structure was found to be increased with adding boron, whereas decreased with adding phosphorus.

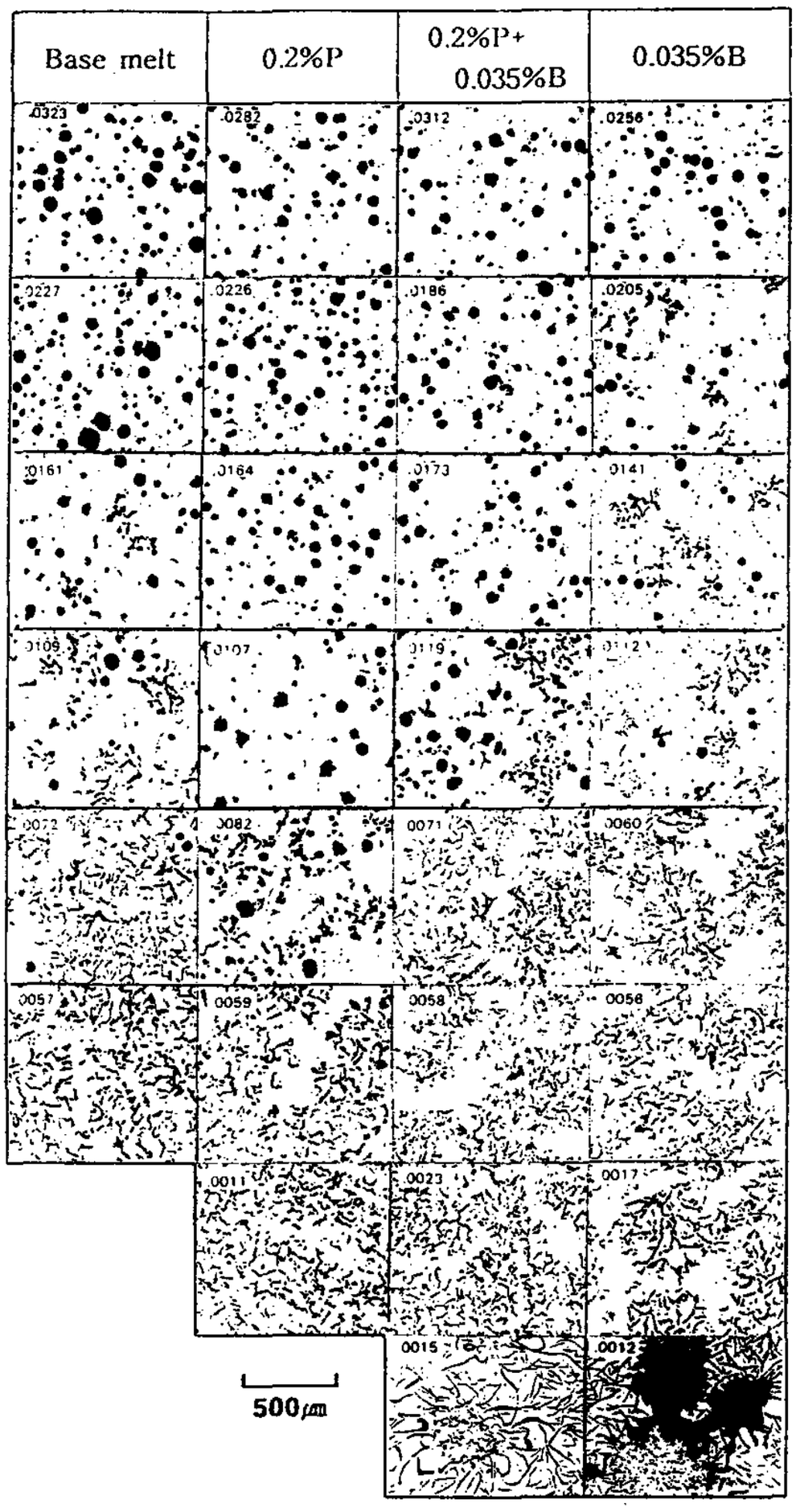

Fig. 3. Changes in graphite morphology with the Mg-Equivalent.

3.2 The influence of alloying elements and cooling rates during solidification on the formation of phosphide eutectics

In a first series of experiments, step-block castings, as shown in Fig.4 with dimensions, were used as test castings for investigating the influence of cooling rates during

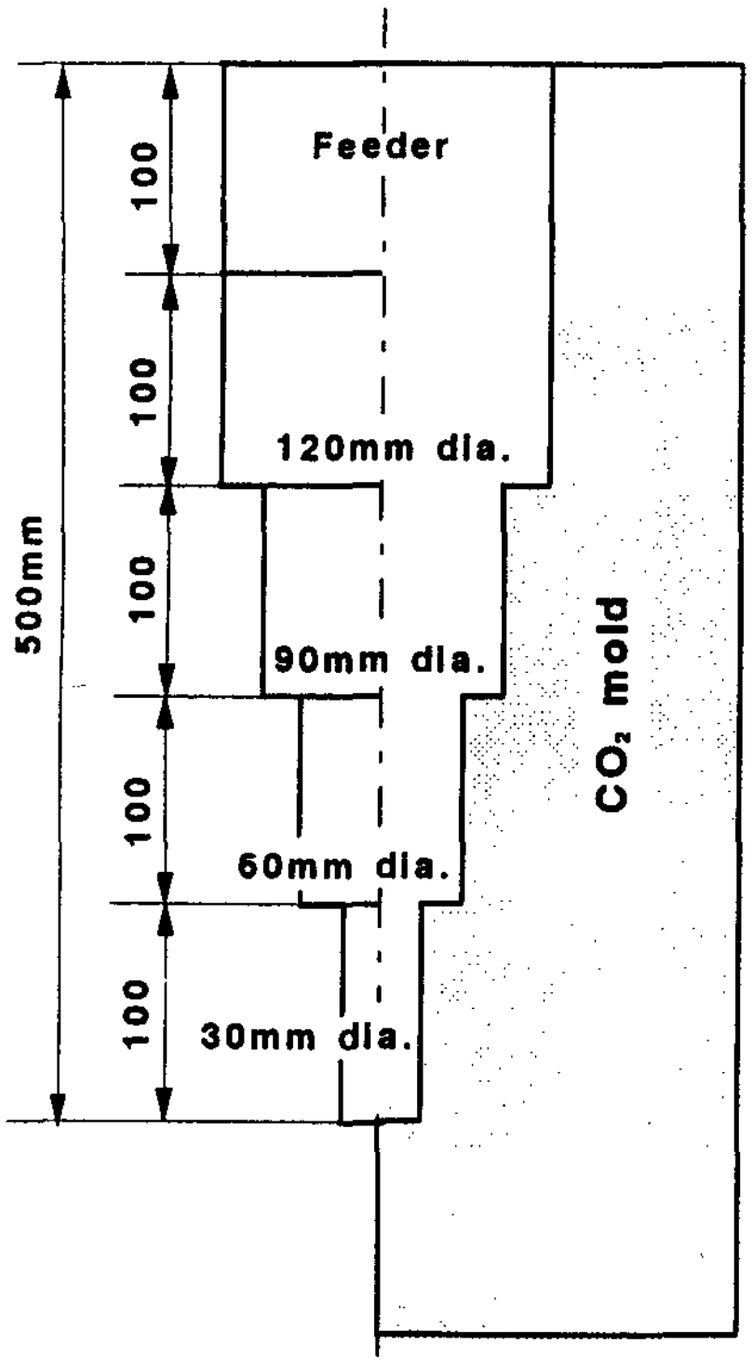

Fig. 4. Dimensional profile of the rounded step-block.

Table 2. Chemical composition of the rounded step-block specimens.

SPECIMEN GROUP	C	Si	Mn	P	S	B	Cu	Sn	Mo	Mg
CV-P	3.84	1.52	0.62	0.20	0.009	—	—	—	—	0.011
CV-PB	3.90	1.43	0.61	0.19	0.011	0.033	—	—	—	0.016
CV-PBA	3.90	1.60	0.66	0.20	0.014	0.037	1.51	0.06	0.20	0.016

solidification on the formation of phosphide eutectics. Pt-Pt13%Rh thermocouples with diameter of 0.5 mm were placed at each center of the step in the casting to obtain a record of cooling curves. The molds were produced using silicate bonded sand. Copper, tin, and molybdenum were added to the melt for producing pearlitic matrix, and also phosphorus for the formation of phosphide eutectics, and boron for increasing the hardness of the phosphides eutectics, were added to the melt, and chemical compositions of this test castings are given in Table 2.

Cooling rates from the pouring temp. to 900℃ were estimated from the recorded cooling curves for each step in the test casting, and they were about 80℃/min for the step with diameter of 30mm, 20℃/min for 60mm, 11℃/min for 90mm, and 10℃/min for 120mm, respectively.

Observations on the microstructure of CV graphites and phosphide eutectics, and the eutectic cell size as a function of alloying elements and diameter of the steps in the test castings are summarised in Fig. 5. The area fraction of phosphide eutectics for CV-PB specimen was found to be higher than that for CV-P specimen, i.e. addition of boron produced a greater increase in phosphide eutectic content in the higher content of phosphorus(0.2%) iron. This is possibly due to increase in the amount of carbide phase rather than graphite phase in the phosphide eutectics, and due to promoting primary carbides that could not be distinguished from phosphide eutectics in observation[24].

The matrix structure of the CV-PBA was fully pearlitic, and the formation of eutectic carbides was found to be supressed compared to the CV-PB specimen. This is attributed to the fact that the addition of Cu which was added for promoting pearlitic matrix, supressed the precipitation of free cementite by increasing the equilibrium eutectic temperature of Fe-graphite and also by decreasing the equilibrium eutectic temperature of Fe-cementite[25]. The addition of copper was found to decrease the tendency of forming ledeburitic carbides in the phosphide eutectic.

The liquidus phosphide eutectic was found to solidify as a pseudo-binary phosphide eutectic($\gamma Fe-Fe_3P$), but with increasing of the cooling rate non-equilibrium phosphide eutectic($\gamma Fe-Fe_3C-Fe_3P$) with needle type carbide could be formed. However, the liquidus phosphide eutectic containing both phosphorus and carbide-forming boron was found to solidify always as a non-equilibrium phosphide eutectic($\gamma Fe-Fe_3C-Fe_3P$) with coarse carbide, independent of cooling rates. Such a transition in microstructure with cooling rates and alloying elements is shown in Fig. 6.

In a second series of experiments, the influence of complementary alloying of Mo, P, and B on the microstructure of graphite and phosphide eutectics were investigated. The target compositions of the CV graphite cast irons were 3.85%C, 1.7%Si, 0.7%Mn, 1.5% Cu, 0.05%Sn, and also containing 0.2, 0.4, 0.6% P, 0.2, 0.4%Mo, and 0.035, 0.07% B, and results of chemical analyses for the specimens are presented in Table 3. Specimens

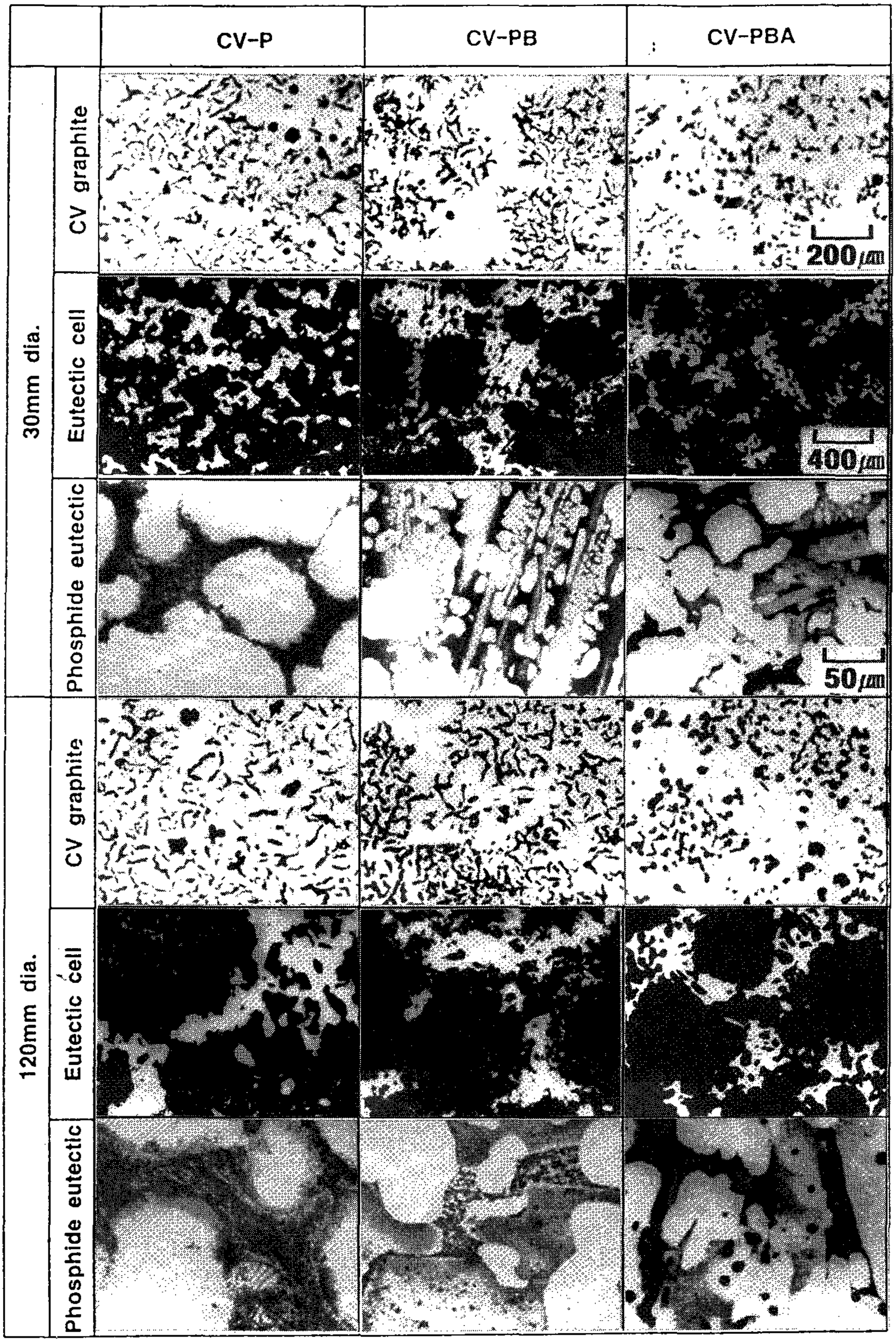

Fig. 5. Variations in microstructure with alloying elements and cooling rates during solidification for P-contained CV graphite cast irons(CV graphite: as polished, Eutectic cell: etched in Steads etchant, Phosphide eutectic: etched in Murakami etchant).

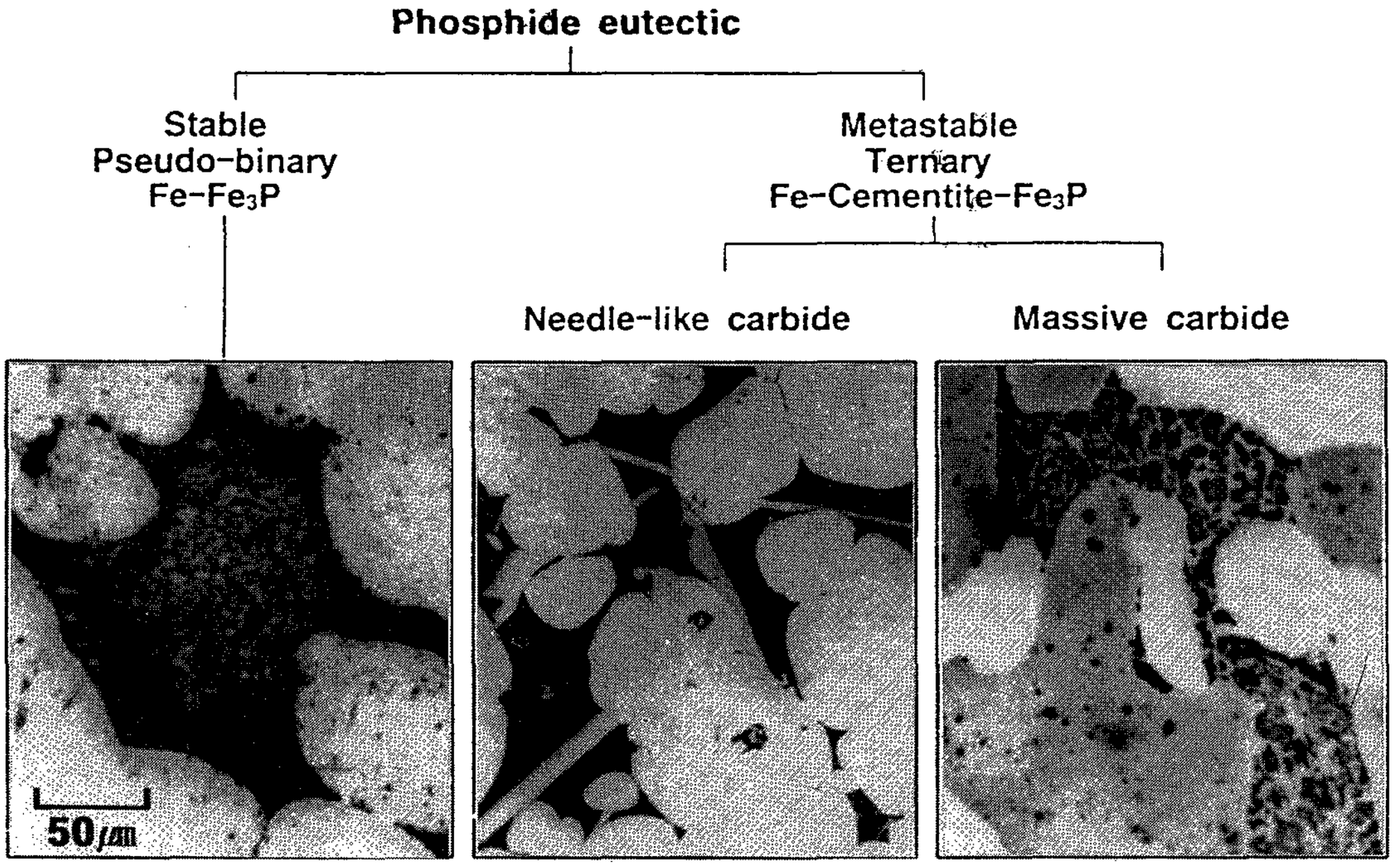

Fig. 6. Changes in microstructure of phosphide eutectics with alloying elements and cooling rates (etched with Murakami etchant).

Table 3. Chemical composition of the specimens.

SPECIMEN GROUP		C	Si	Mn	P	S	Cu	Sn	Mo	B	Al	Mg
A	1	3.92	1.71	0.69	0.224	0.016	1.44	0.06	0.20	0.034	0.021	0.0141
	2	3.92	1.71	0.69	0.396	0.013	1.42	0.06	0.20	0.033	0.019	0.0116
	3	3.87	1.72	0.70	0.635	0.014	1.40	0.06	0.19	0.032	0.017	0.0100
B	4	3.89	1.77	0.66	0.231	0.017	1.44	0.06	0.19	0.066	0.019	0.0165
	5	3.83	1.78	0.69	0.429	0.019	1.44	0.06	0.20	0.065	0.018	0.0170
	6	3.77	1.81	0.70	0.639	0.017	1.43	0.06	0.20	0.064	0.018	0.0163
C	7	3.81	1.70	0.69	0.234	0.019	1.45	0.06	0.38	0.033	0.017	0.0162
	8	3.77	1.68	0.68	0.449	0.022	1.42	0.06	0.38	0.032	0.015	0.0170
	9	3.78	1.71	0.70	0.645	0.018	1.44	0.06	0.40	0.031	0.014	0.0152
D	10	3.78	1.74	0.68	0.239	0.018	1.46	0.06	0.41	0.072	0.020	0.0164
	11	3.78	1.74	0.68	0.395	0.016	1.43	0.06	0.42	0.068	0.019	0.0151
	12	3.78	1.69	0.68	0.636	0.015	1.42	0.06	0.40	0.062	0.019	0.0153

for testing mechanical properties were prepared from the 35mm Y-blocks, which were cast in the silicate bonded sand mold. All of these specimens showed a fully pearlitic matrix, and exhibited a desired compacted vermicular graphite structure with a relatively low Mg-Equivalent of 0.0048-0.0078.

The area fraction of phosphides in phosphide eutectic was found to be increased with an increased amount of phosphorus addition, and the carbides in phosphide eutectic became coarse with increasing of boron and molybdenum addition.

It was also observed that graphite struc-

ture was distributed in a cluster and the growth of eutectic cell size was retarded with an increase in phosphorus, boron and molybdenum content, due to the increased amount of phosphide eutectics formed at the intercellular boundary. However, when the content of phosphorus was constant, with an increase in boron, the area fraction of phosphide eutectics increased, and the area fraction of graphite decreased. This is possibly due to the fact that the excess amount of boron which is beyond the maximum solubility of the matrix, can easily form $Fe_3(CB)$, by consuming a lot of carbon[26].

Fig.7 shows the influence of complementary addition of phosphorus, boron, and molybdenum on the area fraction of graphite(a) and phosphide eutectics(b). According to these figures, the area fraction of graphite and phosphide eutectic increased with an increase in phosphorus, as the phosphorus act as an phosphide former as well as an graphitizer, i. e. reduce the eutectic carbon content.

With an increase in Mo content, the area fraction of phosphide eutectics was increased. This is because the Mo addition lower the phosphorus content of the phosphide phase– in turn, phosphide eutectics– to the extent that there is a considerable increase in volume of phosphide eutectics in the matrix[24, 27].

3.3 The influence of phosphide eutectics on the mechanical properties

With the specimens from the second series of experiments, the influence of phosphide eutectics on the mechanical properties were investigated. Specimens for testing mechanical properties were prepared from the 35mm Y-blocks, which were cast in the silicate bonded sand mold.

The ultimate tensile strength of the specimens was found to be 28.1–40.3kg/mm², depending on their composition. Fig.8 shows the variation of tensile strength with the amount of phosphide eutectics. The tensile strength is decreased with an increase in P, and with an increase in total amount of P, B and Mo addition. From this figure, it could be said that the tensile strength is strongly influenced by the area fraction of phosphide eutectics. This is mainly attributed to the presence of microshrinkage porosity, which is formed by contraction of the phosphorus-rich liquid on

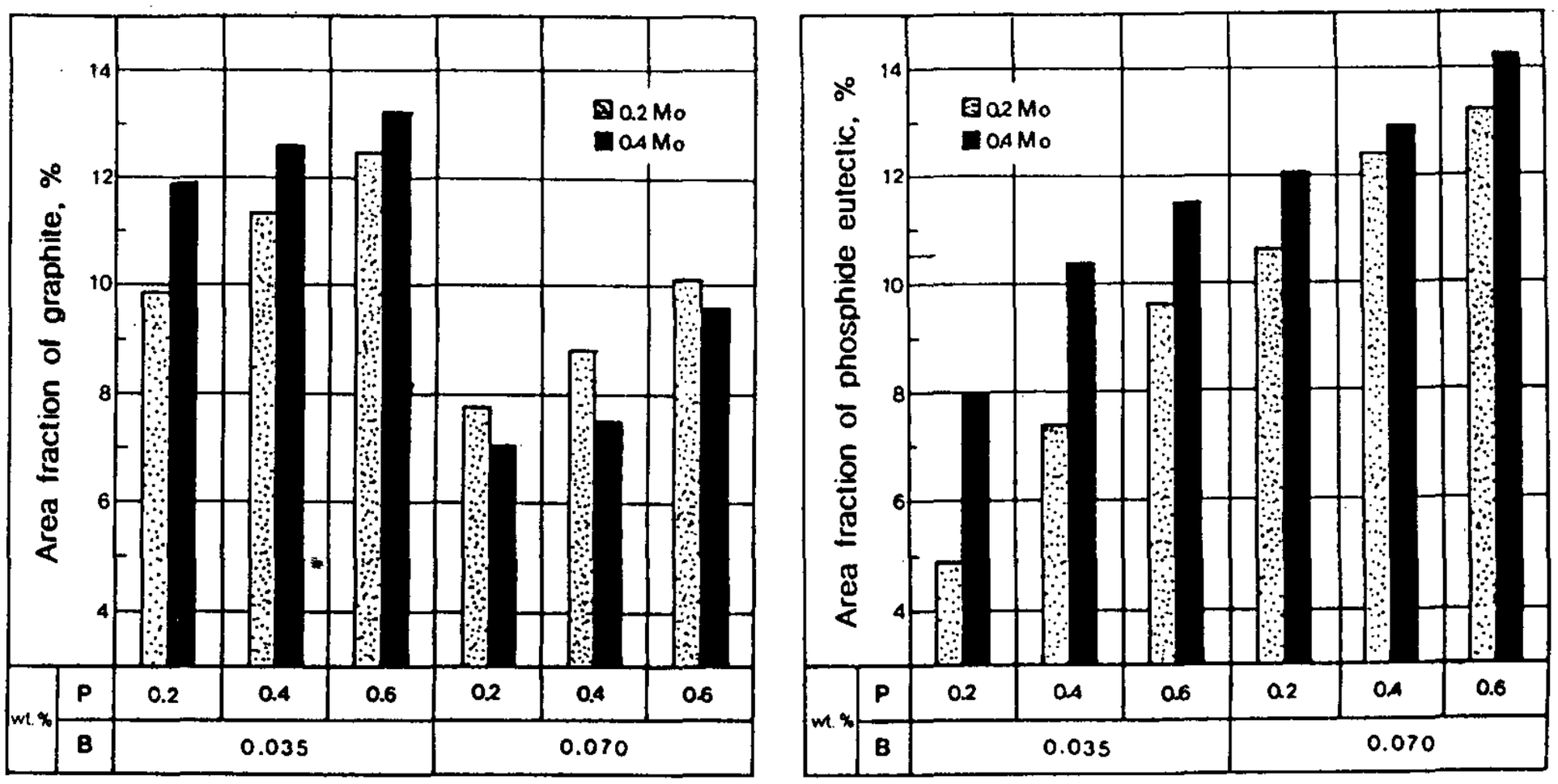

Fig. 7. The influence of alloying elements on the area fraction of (a) graphite and (b) phosphide eutectic.

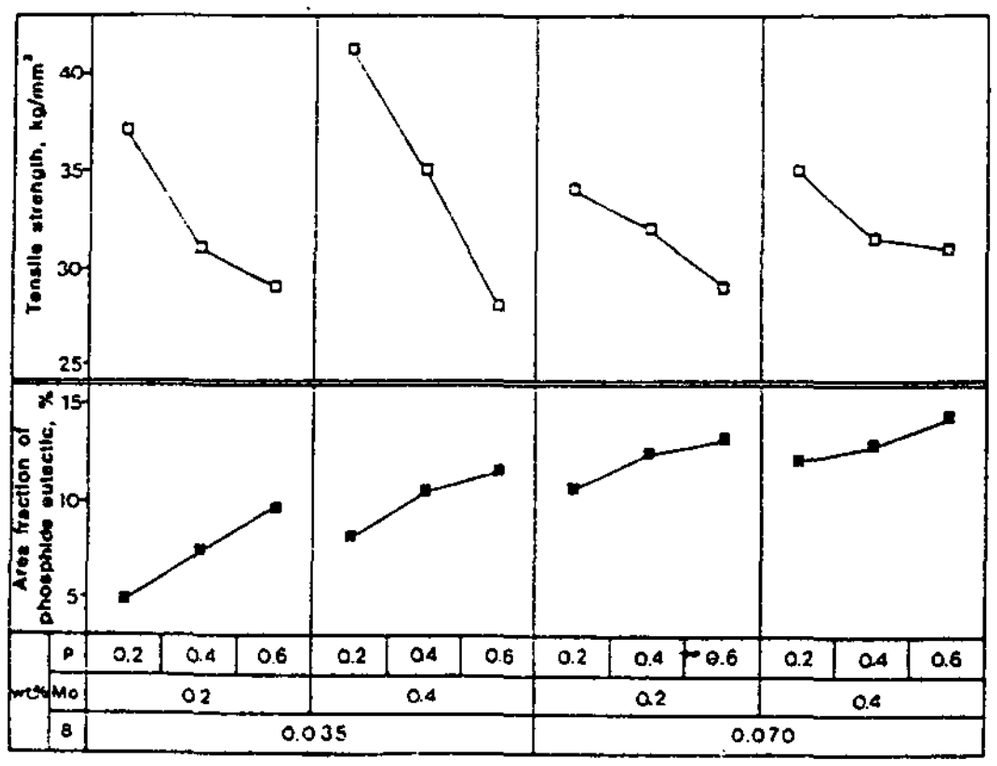

Fig. 8. Variations in tensile strength with the amount of phosphide eutectics.

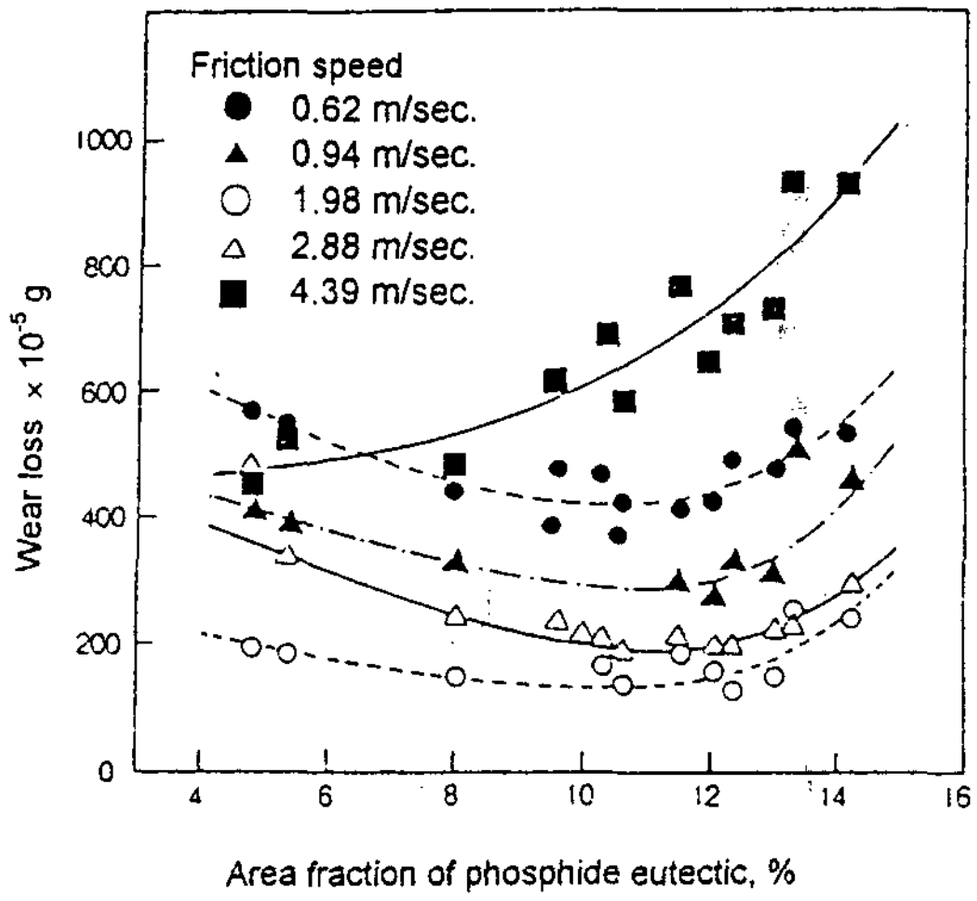

Fig. 9. Variations in amount of wear loss with the area fraction of phosphide eutectics.

cooling from the iron-graphite eutectic to the phosphorus eutectic temperature and by subsequent solidification contraction at the phosphide eutectic temperature[27]. The quantity of shrinkage porosity is generally increased with the amount of phosphide eutectic, and Mo additions tend to greatly magnify the microporosity at a given P content[24]. The microhardness of phosphide eutectic was found to be increased up to about MVH 700 -1200, and the microhardness of pearlitic matrix up to MVH 310-450.

The influence of phosphide eutectic content on the wear property was investigated. Test specimens of 60mmL×25mmW×10mmT were machined and ground on 600 grade emery paper. Wear test were conducted with OGOSHI type tester in dry conditions with a normal load of 6.3kgf for a sliding distance of 600m. The counter surface was a well-ground and hardened steel ring(SCM4 steel, HRc 50) rotated by a motor. The friction velocity was varied with 0.62, 0.94, 1.98, 2.88 and 4.39m/sec.. Before and after the wear runs, samples were weighed accurately using a sensitive balance for wear loss determination.

Fig.9 shows the variation in amount of wear loss with the area fraction of phosphide eutectics under various friction speeds. Considering the wear loss for friction speeds up to 2.88m/s. CV graphite cast irons possessing higher amount of phosphide eutectic exhibit better wear resistance, but the wear loss increase again if the area fraction of phosphide eutectics exceed more than 10%.

However, at a friction speed above 4.39m/s, the amount of wear loss increase continuously with an increase in the amount of phosphide eutectics. This is caused by an increase in the rate of production of oxide brought about by increased frictional heating. The coefficient of friction is higher and the thermal conductivity is lower for phosphide eutectics, so the surface temperature will be increased with increased sliding speed. As the sliding speed is increased heat build up at the surface of the phosphide iron caused thermal softening of the substrate, thus the surface was unable to support the oxide and severe wear occurred. At higher sliding speeds, the frictional heat developed is sufficient to produce a continuous adherent oxide film, and the wear rate becomes increased[20].

4. CONCLUSIONS

1. The fading of Mg by formation of magnesium oxide for the melt with P is slower than for the melt with B, and the melt with B shows higher sulfur reversion than the melt with P. The Mg-Equivalent for producing compacted vermicular graphite structure was found to be decreased with adding P, whereas increased with adding B.

2. The liquidus phosphide eutectic was found to solidify as a pseudo-binary phosphide eutectics ($\gamma Fe-Fe_3P$), but with increasing of cooling rate non-equilibrium phosphide eutectics ($\gamma Fe-Fe_3C-Fe_3P$) with needle type carbide could be formed. However, the liquidus phosphide eutectic containing both P and carbide-forming B was found to solidify always as a non-equilibrium phosphide eutectic($\gamma Fe-Fe_3C-Fe_3P$) with coarse carbide, independent of cooling rates.

3. The area fraction of graphite and phosphide eutectic increased with an increase in P, as the P acted as an phosphide former as well as an graphitizer. However, with an increase in B the area fraction of phosphide eutectics was increased, but the area fraction of graphite was decreased. With an increase in Mo content, the area fraction of phosphide eutectics was increased.

4. The microhardness of phosphide eutectic was found to be increased up to about MVH 700-1200, and that of pearlitic martix being up to MVH 310-450. The ultimate tensile strength of the specimens was found to be 28.1-40.3kg/mm^2, and the tensile strength is decreased with an increase in content of phosphide eutectics.

5. CV graphite cast irons possessing higher amount of phosphide eutectics exhibit better wear resistance for lower friction speed, but the wear loss increase again when the area fraction of phosphide eutectics exceed more than 10%. However, at a higher friction speed, the amount of wear loss increase continuously with an increase in the amount of phosphide eutectics.

5. REFERENCES

[1] H.T.Angus, BCIRA Journal, Vol. 10 (1962), pp610-626.
[2] K.Maruda, Journal of M.E.S.I., Vol. 19 (1984), pp227-234.
[3] B.J.Taylor and T.S.Eyre, Tribology International, Vol.12(1979), pp78-88.
[4] O.Fujita, IMONO, Vol. 34(1962), pp491-501.
[5] I.O.Tsypin, A.A.Cherpov and V.K.Frolov, Translated from Liteinoe Proizvodstvo, Vol.7(1976), pp40-41.
[6] W.Faifhurst and Reohrig, Foundry Trade Journal, Vol. 155(1983), pp104-123.
[7] P.A.Green and A.J.Thomas, AFS Trans, Vol. 87(1979), pp569-572.
[8] K.P.Cooper and C.R.Loper Jr., AFS Trans., Vol. 81(1978), pp241-248
[9] M.J.Lalich and S.J.LaPresta, Foundry M & T, Sept.(1978), pp56-67.
[10] M.Sasaki, K.Taniguchi, C.Yoshida and T. Sakamoto, Imono, Vol. 55(1983), pp219-224.
[11] Y.Tanaka, H.Saito and K.Ikawa, Imono, Vol. 53(1981), pp187-192
[12] G.F.Ruff and B.K.Doshi, Modern Casting, Vol. 70(1980), pp54-57.
[13] K.R.Zigler and J.F.Wallace, AFS Trans., Vol. 92(1984), pp735-748.
[14] V.S.R.Murty, S.Seshan and Kishore, Foundry Trade Journal, Vol.159(1985), pp132-140.
[15] R.R.Oathout, Metal Progress, Vol.114 (1978), pp54-57.
[16] E.Nechtebeger, H.Pure, J.B. von Nesselrode, and A.Nakayama, 49th Int. Foun-

dry Congress, Chicago(1982), pp1-37.
[17] J.F.Wallace, AFS Trans., Vol. 83(1975), pp363-378.
[18] E.N.Pan and C.R.Loper,Jr., AFS Trans., Vol. 94(1986), pp545-556.
[19] T.Hirooka, T.Asikawa and H.Teramura, Imono, Vol. 45(1973), pp488-497.
[20] T.S.Eyre and P.Williams, Wear, Vol. 24 (1973), pp337-349.
[21] H.H.Cornell and C.R.Loper,Jr., AFS Trans,. Vol.93(1985), pp435-442
[22] J.Tartera, AFS Int. Cast Metal J., Vol. 5(1980), pp7-14.
[23] F.D.Richardson, Physical Chemistry of metals in metallurgy 2, Academic Press, N.Y.(1974), pp295.
[24] R.B.Gundlach and W.G.Scholz,AFS Trans., Vol. 81(1973), pp395-402.
[25] J.F.Janowak and R.B.Gundlach, AFS Trans., Vol. 164(1982), pp847-863.
[26] H.I.Park, Y.H.Kim, and M.H.Kim, JUJO, Vol. 9(1989), pp311-319.
[27] P.C.Liu and C.R.Loper, Jr., AFS Trans., Vol. 92(1984), pp289-295.